DOI: 10.21062/mft.2022.057 http://www.journalmt.com

Effect of Higher Iron Content and Manganese Addition on the Corrosion Resistance of AlSi7Mg0.6 Secondary Alloy

Martin Mikolajčík (0000-0002-7477-6237), Eva Tillová (0000-0002-1010-0713), Lenka Kuchariková (0000-0002-2688-1075), Lucia Pastierovičová (0000-0001-5341-9292), Mária Chalupová (0000-0003-0175-9484), Milan Uhríčik (0000-0002-2782-5876), Zuzana Šurdová (0000-0002-4823-2279)
Faculty of Mechanical Engineering, Department of Materials Engineering University of Žilina, Univerzitná 8215/1, 010 26 Žilina, Slovakia. E-mail: martin.mikolajcik@fstroj.uniza.sk

The use of secondary aluminium alloys gives manufacturers in many industries the opportunity to produce their products more economically and environmentally friendly. The secondary aluminium alloy production is sustainable in the long term. As aluminium does not lose its excellent properties through recycling, secondary aluminium alloys have the potential to replace primary aluminium in many applications. However, recycled aluminium alloys have the disadvantage of insufficient sorting and thus a higher content of impurities in their chemical composition. The most common undesirable element in Al-Si-Mg cast alloys is iron. It adversely affects mechanical properties, fatigue behaviour and corrosion resistance. The influence of iron can be reduced by the addition of manganese. This paper deals with the effect of manganese on the morphology of Fe-phases and corrosion resistance of AlSi7Mg0.6 secondary alloy with higher iron content (0.75 % and 1.26 %).

Keywords: AlSi7Mg0.6 cast alloy, Corrosion resistance, Audi test, Higher iron content, Manganese addition

1 Introduction

Al-Si-Mg-based alloys are aluminium alloys widely used in the automotive field because of their good mechanical properties, low density, excellent fluidity, castability and finally - corrosion resistance. The properties of these alloys depend on the morphology and size of the main phase components: α-phase (solid solution of silicon in aluminium), eutectic silicon particles and Fe-rich and Mg-rich intermetallic phases. Of the Fe-phases, the most observed phases in these alloys are phases such as the Al_5FeSi phase with plate/needle-like morphology and the $Al_{15}(FeMnMg)_3Si_2$ phase with skeleton-like or script-like morphology [1]. Al_5FeSi phase is known to be a primary phase, with a three-dimensional form of a thin platelet that looks like needles in a two-dimensional optical micrograph. These platelets are usually potential sites for crack initiation, where eventual breakup failure occurs. Often, Mn is found in secondary metal made from recycled wrought products and is usually not deliberately added to virgin cast alloys. Manganese can transform Fe-rich (Al_5FeSi) phases morphology of Al-Si-Mg alloy from platelets to a more cubic phase ($Al_{15}(FeMn)_3Si_2$ or $Al_{15}(FeMnMg)_3Si_2$) with skeleton-like or script-like morphology and this improves the alloy's ductility and tensile strength [2]. Intermetallic phase Mg_2Si provides the ability to be hardened using heat treatment. Thanks to the Mg_2Si phase, Al-Si-Mg alloys can increase their mechanical and fatigue properties [3]. Also, the corrosion resistance is positively affected by Mg_2Si particles [4].

Al-Si-Mg alloys are mostly used in the automotive industry (engine blocks, cylinder heads, transmissions case etc.), but their castings also find their applications in the aerospace and food industry [5-6]. The usage of aluminium alloy castings in the automotive industry still increases thanks to good castability (low tendency to form shrinkage and cracks) and other properties - weight, strength, workability, and relatively low cost. Aluminium is approximately one-third the density of steel, making it lightweight in comparison [6-8]. As aluminium is also a good electrical conductor, its alloys found application also in the energy production industry [9].

Common aluminium casting processes include die casting, sand casting, casting into shell moulds, permanent mould casting, casting into ceramic moulds, squeeze casting and casting into plaster moulds. When using the squeeze casting method, the metal solidifies under pressure, which results in a significant improvement in the properties of castings [10-13]. Products with smooth surfaces, high dimensional accuracy, the lack of surface defects and good shape fidelity can be made [14].

Secondary aluminium alloys are the materials produced by recycling aluminium scrap. Aluminium alloys are 100 % recyclable without loss of properties. There is no difference in the quality between new and recycled aluminium alloys, so they can be melted and recast over again. Only 5 % of the energy required for

primary aluminium production is needed for the recycling process. This implies that the secondary production of aluminium alloys is economically and environmentally beneficial. Due to this fact, the amount of secondary aluminium increases every year [8, 15-16]. Currently, the predominant use (approx. 70 %) of recycled aluminium is in the production of aluminium-silicon casting alloys mostly used in the automotive industry, with the balance converted to wrought alloys for re-use in sheet or extruded form, with a small proportion being converted to de-oxidant for the steel industry. Many secondary alloys utilized today, especially in the aerospace industry where requirements for exceptionally high ductility and toughness are common, call for very tight composition controls on both Fe and Si. Impurity levels above 0.10 - 0.15 % Fe or 0.15 - 0.25 % Si are unacceptable, for example, in premium high-toughness aerospace alloys. High-performance automotive alloys restrict both Si and Fe to 0.40 % maximum. Both elements (Fe and Si) are difficult to control in recycled metal and tend to increase modestly the more often the metal has been recycled. Elements other than Fe may be expected to gradually increase with time and may require special attention [17-18].

Alloying elements in aluminium alloys are classified as major, minor, microstructure modifiers or impurities. In Al-Si-Mg based alloys major alloying elements are silicon and magnesium. The most used Al-Si-Mg-based casting alloys are AlSi5, AlSi7Mg and AlSi10Mg, which can be used for parts with thin walls and complex geometry. These alloys are also used for parts which are subject to high loads and are complicated in shapes. The common problem of secondary aluminium alloys is the presence of a high amount of iron, which is an impurity element in Al-Si-Mg-based alloys. The content of iron can increase because of using steel tools during the alloying process, and it is also present in bauxite. When aluminium is recycled, it is technologically not possible to remove the iron out of the liquid. This implies, that the amount of iron in the secondary aluminium alloys increases [16-21].

Metal corrosion is the physicochemical interaction of the metal and the environment. It leads to changes in the properties of the metal, which can influence its ability to work properly. The most widely used corrosive environment is the atmosphere. Aluminium and its alloys have a strong affinity for oxygen. That leads to the formation of a passive layer of Al_2O_3 on the surface. The oxide layer protects the material against the continuation of the corrosion process. The thickness of the protective oxide film is about 5 nm. The layer is resistant to attack from water and oxygen in a wide range of temperatures. However, aluminium alloy products are also widely used in other environments, which are chemically more aggressive. Technically significant environments are different soil, the water of the river and saltwater of the sea, which acts aggressively on vessels and ports. The corrosion behaviour of aluminium alloys in these environments is not as good as in the atmosphere (aluminium alloys are attacked by localized forms of corrosion) and it is still needed to be investigated. The main type of corrosion of aluminium alloys is pitting corrosion [1, 22-28].

One of the most important factors causing pitting corrosion of the matrix is the presence of Al_5FeSi intermetallic phases. Al_5FeSi phase is plate-shaped (visible as needle-shaped in the transverse section). These phases are cathodic concerning the aluminium matrix. In addition to the corrosion resistance, the Al_5FeSi phase also harms mechanical properties (decrease of ductility and ultimate tensile strength) and fatigue behaviour. Plate-like Al_5FeSi phase can also influence porosity [6, 29-30].

The effect of iron can be corrected by alloying with a suitably selected corrector, such as Mn, Cr, Be and Ni. The most widely used additive for this purpose is manganese. For secondary aluminium alloys, the recommended alloying ratio of Mn/Fe is 0.5 [6, 30]. The influence of iron can also be reduced with chemical treatment, solid solution hardening and precipitation hardening [30]. There exist a big discrepancy concerning ranges of the temperature and duration of the solutioning and ageing operations, but in general, it can be said that the usual temperature of solutioning is around 535 °C and the temperature of ageing is around 160-170 °C. The parameters depend on the chemical composition of the material [3, 31-32].

This study is focused on the effect of Mn addition on the morphology of Fe-rich intermetallic phases and the evaluation of its shape and distribution in AlSi7Mg0.6 secondary alloy with higher iron content. The work is part of a VEGA project 01/0398/19 aimed at the study of secondary alloys with higher iron content.

2 Experimental part

Secondary aluminium alloy AlSi7Mg0,6 with higher iron content was used as the experimental material. The material was supplied by UNEKO Zátor, a. s. The alloy was cast by gravity casting into sand moulds. The temperature of casting was 750 °C. The ECOSAL Al 113S salt was used for refining. Four melts were cast - alloys A, B, C and D, with similar chemical compositions. The only significant differences were in the iron and manganese content. Alloys A and B had about 0.7 wt.% Fe and alloys designated C and D contained about 1.2 wt.% Fe (Tab. 1).

Tab. 1 *Chemical composition of experimental alloys [wt. %]*

Alloy	Si	Mg	Fe	Mn	Ti	Cu	Al
A	7.374	0.477	**0.750**	0.007	0.121	0.017	ball.
B	7.252	0.501	**0.728**	**0.402**	0.120	0.040	ball.
C	7.276	0.548	**1.264**	0.008	0.117	0.012	ball.
D	7.047	0.546	**1.245**	**0.661**	0.115	0.013	ball.

To determine the effect of Mn, alloys A and C were alloyed with manganese in a ratio of approximately 1:2 relative to the iron content. To increase the iron and manganese content, AlFe75 and AlMn75 pre-alloys were used. The exact chemical composition of the alloys used was determined by the manufacturer UNEKO according to EN 10204 3.1 The material was supplied as rods of circular cross-sections with a diameter of 20 mm and a length of 300 mm. The experimental material was not heat treated so only the effect of manganese could be observed.

Samples of the experimental material for microstructure analysis were prepared by the usual preparation process. The specimen was cut either by saw ATM Brillant 240 and pressed into dentacryl using Struers-CitoPress-1. aluminium alloys were used. The process consists of five steps, which differ in the roughness of the sandpaper, the chemical environment, and the duration of the process. In the final stage, the samples were etched with 0.5 % HF.

Samples for the corrosion Audi test were cleaned with water and degreased with ethanol. Three samples were prepared for each melt (marked X, Y, Z). The dried samples were weighed and dipped in the prepared chemical solution. The chemical solution for the Audi test consists of distilled water, NaCl and HCl. In our case, it was necessary to mix the solution with 1,5 l of distilled water, 30 g of NaCl and 102,5 ml of 35 % HCl. The duration of the test was 2 hours. After this time, samples were removed from the solution and cleaned with distilled water and ethanol. After the samples were dried, they were weighed with analytical weight. The difference in the weight of samples before and after the Audi test shows the corrosion resistance of the material. If the weight loss is large, the corrosion resistance of the material is poor.

The microstructure of the material was observed on a NEOPHOT 32 microscope. Quantitative metallography [33-34] was carried out on an Image Analyzer NIS - Elements 5.0 to quantify Fe-rich phases in samples etched by H_2SO_4. Etching by H_2SO_4 was needed to obtain a suitable contrast of Fe-iron phases. To minimize statistical errors in the determinations, fifty micrographs were assessed; a relative error of less than 0.05 was sought. In the metallographic analysis, the assumption is that the Mn-affects the shape and size of the Fe-phases in the microstructure of AlSiMg0.6.

3 Results and discussion

The microstructure of AlSi7Mg0.6 secondary alloy is documented in Fig. 1. The largest area fraction is represented by the α phase (α-matrix), i.e., the substitutional solid solution of Si in Al, which is precipitated in the form of dendrites. The eutectic in these materials is represented by a mixture of α-matrix and silicon particles (Fig. 1a). In addition to these components, intermetallic phases, especially Fe-rich phases and Mg_2Si phases, are present in the structure of the AlSi7Mg0.6 alloy. Depending on the chemical composition, the Fe-phases are precipitated in the form of needles - the Al_5FeSi phase (Fig. 1b), skeleton-like shapes - the $Al_{15}(FeMnMg)_3Si_2$ phase, or in the shape of Chinese script - also the $Al_{15}(FeMnMg)_3Si_2$ phase (Fig. 1c).

The Fe-phases are light grey to dark grey after etching with 0,5 % HF and black after etching with 96 % H_2SO_4.

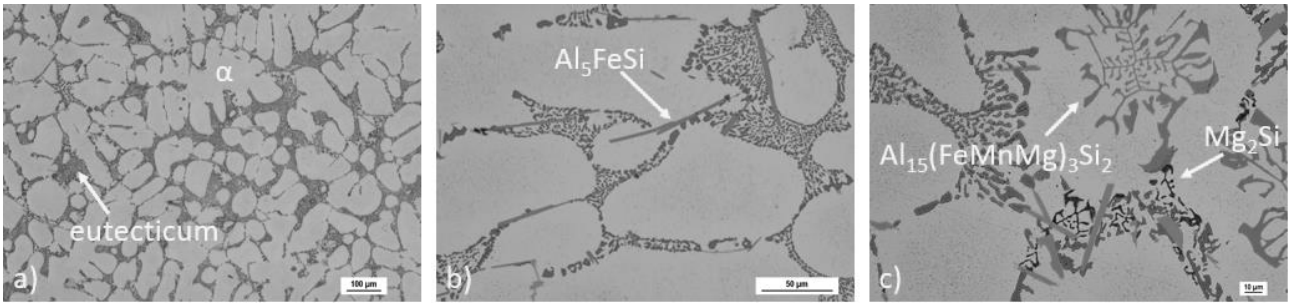

Fig. 1 *Microstructure of AlSi7Mg0.6 secondary alloy, a) basic microstructure, b) detail of Al_5FeSi phase, c) detail of $Al_{15}(FeMnMg)_3Si_2$, etch. 0,5 % HF*

The microstructure of alloys A, B, C and D are documented in Fig. 2. With increasing % Fe and the addition of Mn, the proportion of individual Fe-phases changes. The higher iron content (1.264% and 1.245%, respectively) in alloys C (Fig. 2c) and D (Fig. 2d), compared to alloys A (Fig. 2a) and B (Fig. 2b), results in the formation of more Fe-phases in the structure. In the microstructure of alloys, A and C, the

iron-rich intermetallic phases are excluded in the needle-like shapes of varied sizes (Fig. 2a, Fig. 2c). With higher iron content, the length and amount of needle-like Al_5FeSi phases increase. In alloys with higher manganese content (alloys B and D), the Fe- phases preferentially form skeleton-like shapes and Chinese script (Fig. 2b, Fig. 2d). The needle-like Al_5FeSi phase is observed only locally. In alloy D the $Al_{15}(FeMnMg)_3Si_2$ phase forms large formations.

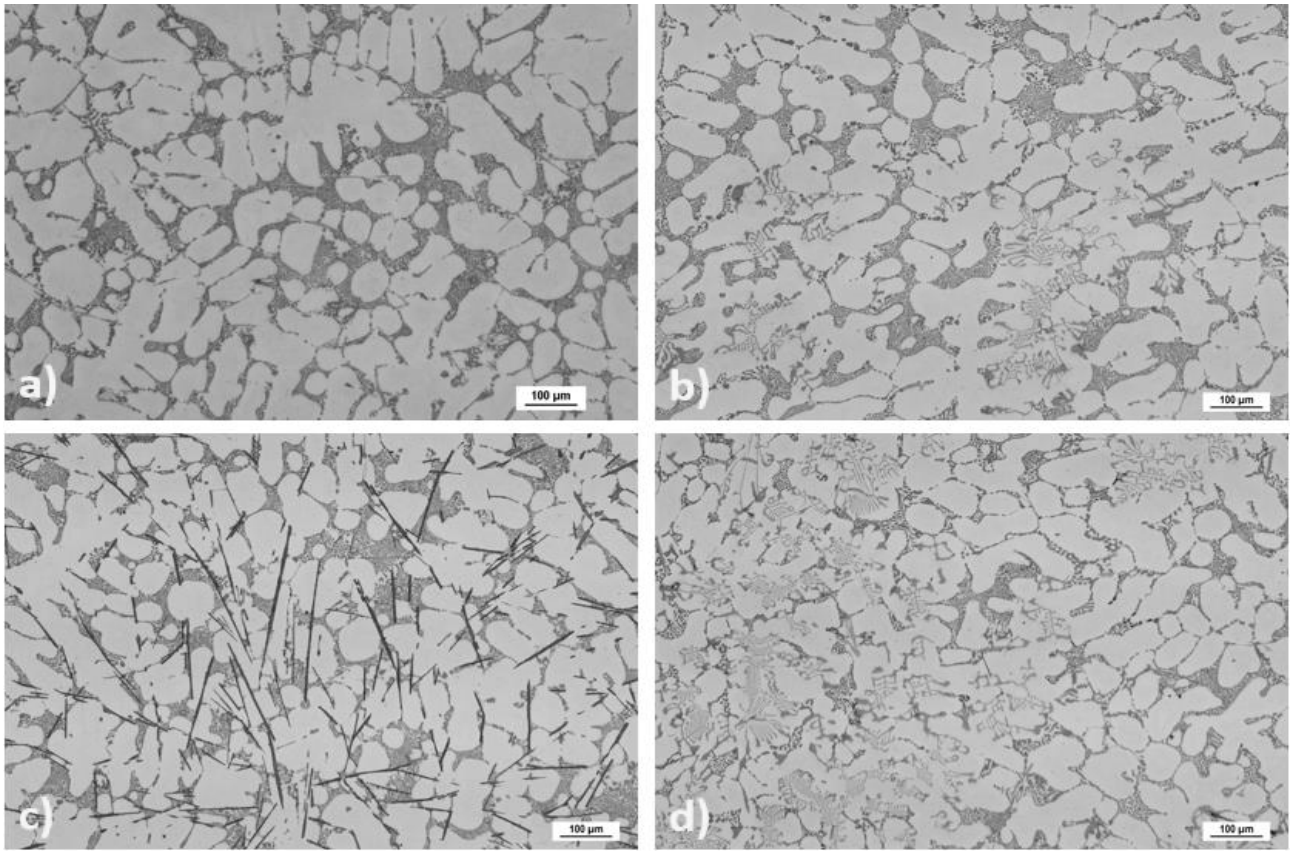

Fig. 2 *Effect of Fe and Mn on the microstructure of experimental alloys, a) alloy A - 0.75 % Fe; b) alloy B - 0.728 % Fe + 0.402 % Mn; c) alloy C - 1.264 % Fe; d) alloy D - 1.245 % Fe + 0.661 % Mn; etch. H_2SO_4*

Eutectic silicon in the alloys studied is precipitated in the form of rods, which are visible as angular grains in the plane of cut (Fig. 2). The marked angular grains are found at the boundaries of the α-phase dendrites. In the centre of the eutectic, the Si has a rounder shape. The shape of the Si particles does not vary from alloy to alloy. A change in their shape could be achieved by modification with a suitably chosen modifier or by heat treatment.

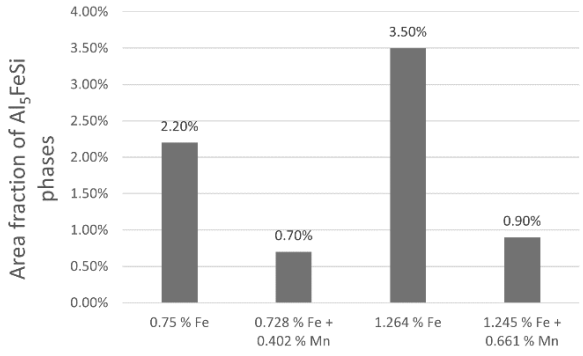

Fig. 3 *Effect of Fe and Mn on the area fraction of Al_5FeSi phases in the AlSi7Mg0.6 alloy*

The results of the quantitative assessment of the area fraction of the Al_5FeSi phase and its length are documented in Fig. 3 and Fig. 4. Al_5FeSi plate/needle-like phases are formed in AlSi7Mg0.6 alloys, especially in the absence of manganese in the chemical composition (Fig. 2a, Fig. 2c). In alloys B and D, which have been doped with manganese to correct the effect of iron, in a ratio of about Fe: Mn/2:1, the iron phases in the form of plates are precipitated in much smaller amounts (in both alloys it is less than 1 % - Fig. 3). At the same time, in the absence of manganese, the area fraction of needle phases in the structure increases with increasing iron content from 2.2 % to 3.5 %.

The addition of manganese also affects the length of the Al_5FeSi-phases (Fig. 4). At an iron content of 0.75 %, the length decreased by about 55 % (from 45.93 µm to 20.28 µm), and for an iron content of about 1.25 %, a decrease of about 20 % (from 46.39 µm to 37.25 µm) was measured. The higher iron content in manganese alloyed alloys causes the formation of longer Al_5FeSi needles. In the case of alloys without manganese (alloys A and C), the effect of iron content on needle length is negligible (45.83 µm and 46.39 µm).

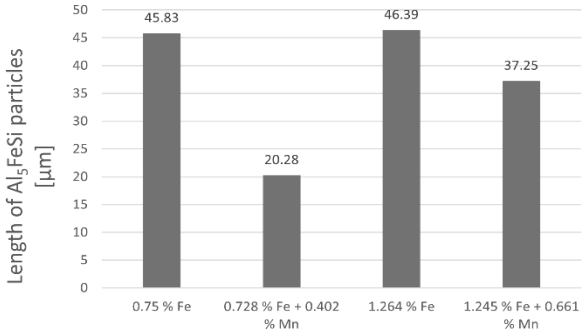

Fig. 4 *Effect of Fe and Mn on the length of Al_5FeSi particles in the AlSi7Mg0.6 alloy*

The effect of iron content on the thickness of Al_5FeSi phases was also observed. The effect is more pronounced in alloys without manganese and with higher iron contents. In the case of manganese alloyed alloys, this fact does not apply.

The presence of manganese in alloys B and D significantly increases the amount of skeleton-like or script-like phases ($Al_{15}(FeMnMg)_3Si_2$), which are created preferably. Because manganese is only present in negligible amounts in alloys A and C, phases with the given morphology are not found in the microstructure of these alloys - Fig. 2.

The aim of the immersion corrosion resistance test (AUDI test) in a prepared solution (HCl + NaCl + water) was to investigate the effect of the iron and manganese content in the chemical composition on the corrosion resistance of AlSi7Mg0.6 alloys based on the mass loss of the samples. Based on the measured data (Fig. 5), it can be evaluated that the corrosion resistance decreases with increasing iron content. Higher weight drops were observed. The correction of the negative effect of iron by manganese affects the improvement of corrosion resistance. Alloy B, which has lower iron content and is also alloyed with manganese, has the highest corrosion resistance. The highest weight loss was observed on samples of alloy C, which has higher iron content in its chemical composition and no manganese.

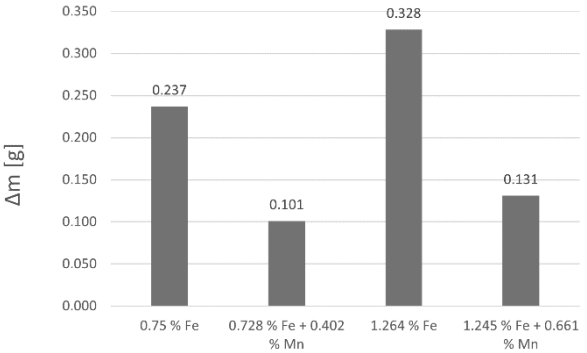

Fig. 5 *Effect of Fe and Mn on the corrosion resistance of AlSi7Mg0.6 alloy*

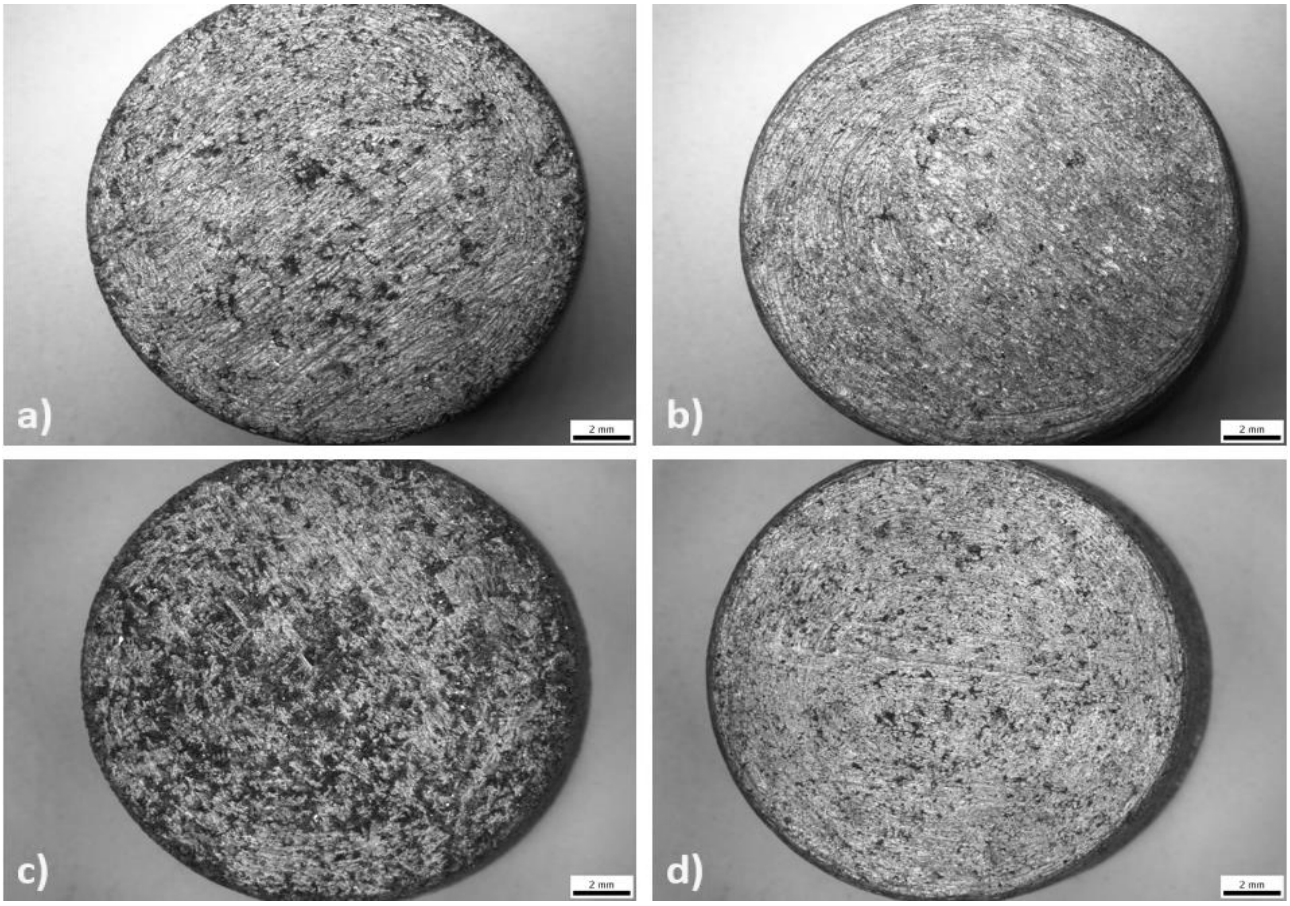

Fig. 6 *Effect of Fe and Mn on corrosion attack rate, a) alloy A - 0.75 % Fe; b) alloy B - 0.728 % Fe + 0.402 % Mn; c) alloy C - 1.264 % Fe; d) alloy D - 1.245 % Fe + 0.661 % Mn*

Iron harms corrosion resistance because it forms the $FeAl_3$ compound, which breaks the continuity of the passive oxide layer. On the other hand, manganese has a positive impact thanks to its ability to form compounds with iron. It helps to reduce its negative effect.

After the Audi test, uneven pitting corrosion of the surface is visible (Fig. 6). An aggressive solution causes the dissolution of the passive layer of aluminium. The thickness of the passive layer depends on the number of inhomogeneities on the surface of the samples. The number of structural inhomogeneities on the surface increases with higher content of iron (Fig. 6a, Fig. 6c).

That is the reason the passive layer of alloy C (higher iron content with no addition of manganese) dissolves the fastest (Fig. 6c). It also means that the corrosion has been developed the deepest in alloy C. The addition of manganese causes higher resistance of the passive layer (Fig. 6b, Fig. 6d). The places where corrosion attack has developed are the dark points in Fig. 6 and Fig. 7.

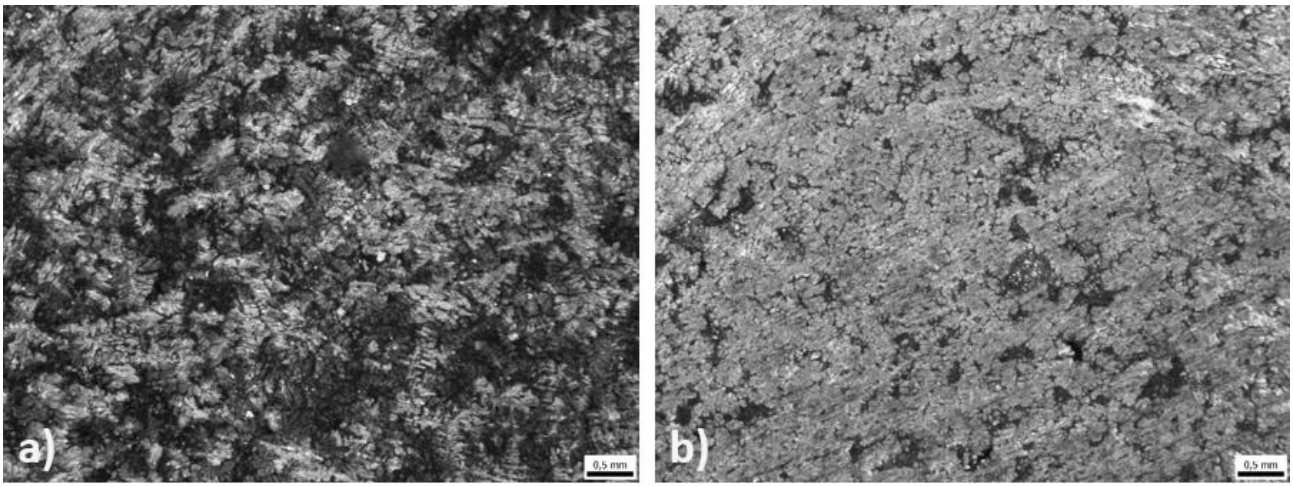

Fig. 7 *Effect of Mn on the corrosion resistance of AlSi7Mg0.6 alloy - detail of pitting corrosion, a) alloy C - 1.264 % Fe; b) alloy D - 1.245 % Fe + 0.661 % Mn*

4 Conclusion

Like all aluminium alloys, Al-Si-Mg-based alloys have high corrosion resistance. The main reason for the good corrosion behaviour is the ability of aluminium to form a passive oxide layer on the surface. Thanks to the layer, these materials have extraordinary corrosion resistance in the atmosphere. However, in more aggressive environments aluminium alloys are subject to corrosion like other metallic materials.

Fast gravimetric corrosion test (after AUDI test) showed that Al-Si-Mg based alloys with higher content of iron are more likely to corrode. The corrosion develops at the places, where the passive layer is breached. Needle/plate-like Al_5FeSi phases are most likely to be the areas, where the corrosion process starts. Pitting corrosion is a dangerous type of corrosion because it attacks the material to a great depth below the surface.

The addition of manganese improves the corrosion properties of Al-Si-Mg-based alloys by elimination of needle-like Al_5Fesi phases and by the formation of skeleton-like or script-like phases ($Al_{15}(FeMnMg)_3Si_2$). The increase of corrosion resistance due to manganese addition is more significant at higher iron content. For secondary aluminium alloys, the recommended alloying ratio of Mn/Fe is 0.5. While using this ratio, the highest corrosion resistance is achieved.

Acknowledgement

The research was supported by the Scientific Grand Agency of the Ministry of Education of Slovak Republic and Slovak Academy of Sciences, VEGA 09/0398/19, KEGA 016ŽU-4/2020, the project to support young researchers at UNIZA, ID project 12715 (Kucharikova) and project 313011ASY4 „Strategic implementation of additive technologies to strengthen the intervention capacities of emergencies caused by the COVID-19 pandemic".

References

[1] ARRABAL, R., MINGO, B., PARDO, A., MOHEDANO, M., MATYKINA, E., RODRÍGUEZ, I. (2013). Pitting corrosion of rheocast A356 aluminium alloy in 3.5 wt.% NaCl solution. In: *Corrosion Science*, Vol. 73, pp. 342 - 355. ISSN 0010-938X

[2] EBHOTA, W.S., TIEN-CHIEN, J. (2018). Intermetallics Formation and Their Effect on Mechanical Properties of Al-Si-X Alloys. In: *Intermetallic Compounds - Formation and*

Applications. London: IntechOpen. ISBN 978-1-83881-298-0

[3] SKOČOVSKÝ, P., BOKŮVKA, O., KONEČNÁ, R., TILLOVÁ, E. (2014). *Náuka o materiáli*, pp. 271 - 278. EDIS-vydavateľstvo ŽU, Žilina. ISBN 978.80-554-0871-2

[4] HOSOVÁ, K., KUBÁSEK, J., STRAKOVÁ, M., NEČAS, D. (2020). Material Properties of Firefighter Ladder Composed from AA6063 and Few Other Aluminium-Based Alloys. In: *Manufacturing Technologies*, Vol. 20, No. 6, pp. 748 - 754. ISSN 1213-2489

[5] SVOBODOVA, J., LUNAK, M., LATTNER, M. (2019). Analysis of the Increased Iron Content on the Corrosion Resistance of the AlSi7Mg0,3 Alloy Casting. In: *Manufacturing Technology*, Vol. 19, No. 6, pp. 1041 - 1046. ISSN 1213-2489

[6] PODPROCKÁ, R., BOLIBRUCHOVÁ, D. (2017). Iron Intermetallic Phases in the Alloy Based on Al-Si-Mg by Applying Manganese. In: *Archives of Foundry Engineering*, Vol. 17, No. 3, pp. 217 - 221. ISSN 2299-2944

[7] KUCHARIKOVÁ, L., TILLOVÁ, E., PASTIRČÁK, R., UHRÍČIK, M., MEDVECKÁ, D. (2019). Effect of Wall Thickness on the Quality of Casts from Secondary Aluminium Alloy. In: *Manufacturing Technology*, Vol. 19, No. 5, pp. 797 - 801. ISSN 1213-2489

[8] MINCIUNA, M. G., VIZUREANU, P., JEŻ, B., SANDU, A. V., NABIAŁEK, M., ACHITEI, D. C. (2022). Correlation between Microstructure and Electrochemical Properties of Al-Si Alloys. In: *Archives of Metallurgy and Materials*, Vol. 67, No. 3, pp. 1067 - 1070. ISSN 1733-3490

[9] POLOCZEK, Ł., DYBOWSKI, B., RODAK, K., JAROSZ, R., KIEŁBUS, A. (2015). Influence of Age Hardening Parameters on the Microstructure and Properties of the AlSi7Mg Sand Cast Alloy. In: *Archives of Metallurgy and Materials*, Vol. 60, No. 4, pp. 3035 - 3041. ISSN 1733-3490

[10] The Advantages of Using Cast Aluminum. (2021). Available online at: https://www.tfgusa.com/cast-aluminum-advantages/

[11] ZYSKA, A., BOROŃ, K. (2021). Comparison of the Porosity of Aluminum Alloys Castings Produced by Squeeze Casting. In: *Manufacturing Technology*, Vol. 21, No. 5, pp. 725 - 734. ISSN 1213-2489

[12] VANKO, B., STANČEK, L. (2012). Utilization of heat treatment aimed to spheroidization of eutectic silicon for silumin castings produced by squeeze casting. In: *Archives of foundry engineering*. Vol. 12, Iss. 1, pp. 111-114. ISSN 1897-3310

[13] STANČEK, L., VANKO, B., BATYŠEV, A. I. (2014). Structure and properties of silumin castings solidified under pressure after heat treatment. In: Metal Science and Heat Treatment, vol. 56, No. 3-4, pp. 197 - 202

[14] ZYSKA, A., KONOPKA, Z., . ŁAGIEWKA, M., NADOLSKI, M. (2013). Optimization of Squeeze Parameters and Modification of AlSi7Mg Alloy. In: Archives of Foundry Engineering, Vol. 13, No. 2, pp. 113 - 116. ISSN 2299-2944

[15] BEHESHTI, R. (2017). *Suitanable Aluminium and Iron Production*. KTH Royal Institute of Technology, Stockholm. ISBN 978-91-7729-214-2

[16] *EAA*_recycling *brochure*: RECYCLING ALUMINIUM A PATHWAY TO A SUSTAINABLE ECONOMY (2015), https://european-aluminium.eu/resource-hub/recycling-aluminium-a-pathway-to-a-sustainable-economy/

[17] KUCHARIKOVÁ, L., TILLOVÁ, E., BOKŮVKA, O. (2016). Recycling and properties of recycled aluminium alloys used in the transportation industry. In: *Transport Problems*, vol. 11, No. 2, pp. 117 - 122

[18] *WWR_Aluminum Cast Alloys. Casting* (Metalworking). Alloy, https://www.scribd.com/document/137004346/WWR-AluminumCastAlloys

[19] APELIAN, D. (2009). *Aluminum Cast Alloys*: Enabling Tools for Improved Performance, pp. 6. North American Die Casting Association, Wheeling, Illinois

[20] MICHNA, Š., LUKÁČ, I., OČENÁŠEK, V., KOŘENÝ, R., DRÁPALA, J., SCHNEIDER, H., MIŠKUFOVÁ, A., et al. (2005). *Encyklopedie hliníku*, pp. 176 - 177. Adin, s. r. o., Prešov. ISBN 80-89041-88-4

[21] DOBKOVSKA, A., ADAMCZYK - CIEŚLAK, B., MIZERA, J., KURZYDŁOWSKI, K. J., KIEŁBUS, A. (2016). The Comparison of the Microstructure and Corrosion Resistance of Sand Cast Aluminum Alloys. In: *Archives of Metallurgy and Materials*, Vol. 61, No. 1, pp. 209 - 212. ISSN 1733-3490

[22] KUSMIERCZAK, S., HREN, I. (2019). Influence of AlSi7Mg0,3 Alloy Modification on Corrosion Behaviour in the Salt Environment. In: *Manufacturing Technology*, Vol. 19, No. 5, pp. 802 - 806. ISSN 1213-2489

[23] KUCHARIKOVÁ, L., LIPTÁKOVÁ, T., TILLOVÁ, E., BONEK, M., MEDVECKÁ, D. (2020). Corrosion Behaviour Correlation of the Secondary Aluminium Casts in Natural Atmosphere and Laboratory Conditions. In: Archives of Metallurgy and Materials, Vol. 65, No. 4, pp. 1455 - 1462. ISSN 1733-3490

[24] KUCHARIKOVÁ, L., et al. (2018). Role of Chemical Composition in Corrosion of Aluminum Alloys. In: *Materials*, Vol. 8, No. 8, pp. 1 - 13. ISSN 2075-4701

[25] BERLANGA-LABARI, C., BIEZMA-MORALEDA, M. V., RIVERO, P. J. (2020). Corrosion of Cast Aluminum Alloys: A Review, In: *Metals*, Vol. 10, No. 10, 1384

[26] FOUSOVA, M., et al. (2019). Corrosion of 3D-Printed AlSi9Cu3Fe Alloy. In: *Manufacturing Technology*, Vol. 19, No. 1, pp. 29 - 36. ISSN 1213-2489

[27] GOMES, L. F., KUGELMEIER, C. L., GARCIA, A., DELLA ROVERE, C. A. & SPINELLI, J. E. (2021). Influences of alloying elements and dendritic spacing on the corrosion behaviour of Al-Si-Ag alloys, In: *Journal of Materials Research and Technology*, 15, pp. 5880-5893

[28] CECCHEL, S., CORNACCHIA, G., GELFI, M. (2018). A study of a non-conventional evaluation of results from salt spray test of aluminum High Pressure Die Casting alloys for automotive components, In: *Materials and Corrosion*, Vol. 70, No. 1, pp. 70-78

[29] ARRABAL, R., MINGO, B., PARDO, A., MOHEDANO, M., MATYKINA, E., MERINO, M. C., RIVAS, A. (2015). Microstructure and corrosion behaviour of A356 aluminium alloy modified with Nd. In: *Materials and Corrosion*, Vol. 66, No. 6, pp. 535 - 541. WILEY-VCH Verlag GmbH & Co. KGaA, Weinheim

[30] PODPROCKÁ, R., BOLIBRUCHOVÁ, D. (2018). The Role of Manganese in the Alloy Based on Al-Si-Mg with Higher Iron Content. In: *Manufacturing Technology*, Vol. 18, No. 4, pp. 650 - 654. ISSN 1213-2489

[31] PEZDA, J., JARCO, A. (2016). Effect of T6 Heat Treatment Parameters on Technological Quality of the AlSi7Mg Alloy. In: *Archives of Foundry Engineering*, Vol. 16, No. 4, pp. 95 - 100. ISSN 2299-2944

[32] HURTALOVÁ, L., TILLOVÁ, E., CHALUPOVÁ, M. (2015). Possibilities of Fe-rich phases elimination with using heat treatment in secondary Al-Si-Cu cast alloy. In: *Metalurgija*, Vol. 54, No. 1, pp. 39 - 42. ISSN 0543-5846

[33] BORKO, K.; TILLOVÁ, E.; CHALUPOVÁ, M. (2016). The Impact of Sr Content on Fe - Intermetallic Phase's Morphology Changes in Alloy AlSi10MgMn. In: *Manufacturing Technology*, Vol. 16, No. 1, pp. 20-6

[34] VAŠKO, A., MARKOVIČOVÁ, L., ZATKALÍKOVÁ, V. & TILLOVÁ, E. 2014. Quantitative Evaluation of Microstructure of Graphitic Cast Irons. In: *Manufacturing Technology*, 14, pp. 478-82